

Power Supply and Consumption Co-Optimization of Portable Embedded Systems with Hybrid Power Supply

Xue Lin¹, Yanzhi Wang¹, Naehyuck Chang², and Massoud Pedram¹

¹Dept. Electrical Engineering, University of Southern California, Los Angeles, CA, USA

²Dept. Electrical Engineering, Korea Advanced Institute of Science and Technology, Daejeon, Korea

¹{xuelin, yanzhiwa, pedram}@usc.edu, ²naehyuck@cad4x.kaist.ac.kr

Abstract—Energy efficiency has always been an important design criterion for portable embedded systems. To compensate for the shortcomings of electrochemical batteries such as low power density, limited cycle life, and the rate capacity effect, supercapacitors have been employed as complementary power supplies for electrochemical batteries, i.e., hybrid power supplies comprised of batteries and supercapacitors have been proposed. In this work, we consider a portable embedded system with a hybrid power supply and executing periodic real-time tasks. We perform system power management from both the power supply side and the power consumption side to maximize the system service time. Specifically, we use feedback control for maintaining the supercapacitor energy at a certain level by regulating the discharging current of the battery, such that the supercapacitor has the capability to buffer the load current fluctuation. At the power consumption side, we perform task scheduling to assist supercapacitor energy maintenance. Experimental results demonstrate that the proposed joint optimization framework of task scheduling and power supply control successfully prolongs the total service time by up to 57%.

I. INTRODUCTION

Maximizing energy efficiency has always been one of the critical design challenges for portable embedded systems, due to the fact that the increase in the volumetric/gravimetric energy density of rechargeable batteries has been much slower than the increase in the power demand of these systems. Techniques such as dynamic power management (DPM) [1], [2] and dynamic voltage and frequency scaling (DVFS) [3], [4] have proven quite effective for minimizing energy consumption. These techniques focus on reducing the energy consumption of the processing units while meeting the performance constraints.

Another path to maximizing energy efficiency lies in the optimization of the power supply units. Due to high energy density and low self-discharge rate, electrochemical batteries have long been used for power supply in portable embedded systems. However, batteries have the shortcomings such as low power density, limited cycle life, and the rate capacity effect, which significantly degrades their efficiency under high load current. Portable systems commonly exhibit large fluctuation in load current, which defies the maximum capacity of batteries. A typical portable system determines the battery size based on

its average power consumption, and thus large fluctuation in load current can significantly shorten the battery service time.

Besides electrochemical batteries, supercapacitors (also called electrical double layer capacitors) are widely exploited for electrical energy storage and power supply. Compared with batteries, supercapacitors exhibit superior efficiency, high power density, and long cycle life. However, they also show disadvantages such as low energy density and high self-discharge rate. Therefore, as electrical energy storage and power supply devices, batteries and supercapacitors have their unique advantages and disadvantages. To overcome the shortcomings of a single type of energy storage device, HEES (hybrid electrical energy storage) systems have been proposed, which are comprised of two or more types of energy storage devices. A simple structure of HEES systems can be found in advanced electrical vehicles, especially for regenerative braking systems [5]. The generalized HEES systems were introduced in [6], [7].

In this work, we consider a portable embedded system with a hybrid power supply and executing periodic real-time tasks. We perform system power management from both the power supply side and the power consumption side to maximize the system service time. Specifically, we use feedback control for maintaining the supercapacitor energy at a certain level by regulating the discharging current of the battery, such that the supercapacitor has the capability to buffer the load current fluctuation. On the other hand, at the power consumption side we perform task scheduling to assist supercapacitor energy maintenance. Experimental results demonstrate that the proposed joint optimization framework of task scheduling and power supply control successfully prolongs the total service time by up to 57%.

II. RELATED WORK

Energy storage and power supply for portable embedded systems has unique requirements, such as size/weight limit, high energy density, high power capacity, and simple structure and control policy. A battery-supercapacitor hybrid power supply is a promising candidate for addressing the above-mentioned requirements. It has a simple architecture, high energy density due to the usage of Li-ion battery, and high power capacity by using supercapacitor as an intermittent energy buffer. Shin et al introduced a battery-supercapacitor hybrid power supply using a constant-current charger to regulate

This work is supported in part by a grant from National Science Foundation, and the Mid-Career Researcher Program and the International Research & Development Program of the NRF of Korea.

the battery output current and considering the energy density constraint of the hybrid power supply in a portable system [8]. To address a similar problem, early work [9] used dual-battery as the hybrid power supply for a portable embedded system in order for exploiting both the rate capacity effect and the relaxation-induced recovery effect. It maximized the utilization of battery capacity under a performance constraint using continuous-time Markov decision process.

Another interesting application of the battery-supercapacitor hybrid power supply is to extend the life time of wireless sensor nodes with energy harvesting [10], [11]. By relying mostly on the supercapacitor as an energy buffer and reducing the charging/discharging frequency of the battery, the wireless sensor nodes can achieve near-perpetual operation. Mirhoseini et al presented HypoEnergy, a framework for extending the lifetime of battery-supercapacitor hybrid power supply, given a preemptively known workload [12]. The same authors further extended their work to the setup with multiple supercapacitors and workload that is not given *a priori* [13] and they used the reinforcement learning technique to derive a near-optimal adaptive management policy. A recent work proposed to use a model-free reinforcement learning technique for an adaptive dynamic power management (DPM) framework in embedded systems with bursty workload and using a hybrid power supply comprised of Li-ion batteries and supercapacitors [14].

III. SYSTEM MODELS

In this work, we consider a portable embedded system with a hybrid power supply and executing periodic real-time tasks. We perform joint control and optimization of charging/discharging of the hybrid power supply with task scheduling in the embedded system. The system architecture is shown in Fig. 1, where the battery is the main energy storage device for the embedded processing unit while the supercapacitor serves as an energy buffer. The battery is connected to the supercapacitor through a charger, which regulates the supercapacitor charging current. The supercapacitor is connected to the embedded processing unit through a power converter, which regulates the supply voltage of the processing unit. This architecture can provide higher energy efficiency than the DC bus based general HEES structure in [6] because fewer converters/chargers are used in this architecture. The voltage and current notations are shown in Fig. 1. The open-circuit voltage (OCV) and closed-circuit voltage (CCV) of the battery are denoted by $V_{bat}^{OC}(t)$ and $V_{bat}(t)$, respectively, whereas the battery discharging current is $I_{bat}(t)$. The supercapacitor terminal voltage, input current, and output current are denoted by $V_{cap}(t)$, $I_{cap,in}(t)$, and $I_{cap,out}(t)$, respectively. The voltage and current levels of the processing unit are denoted by V_{load} (a fixed value) and $I_{load}(t)$, respectively. In the following we will introduce the accurate component models of the portable embedded system, including the battery, the supercapacitor, the charger/converter and the processing unit.

A. Battery Model

We employ the Li-ion battery in the embedded system. We use an electronic equivalent circuit model in [15] for the Li-ion battery model, which is suitable for developing

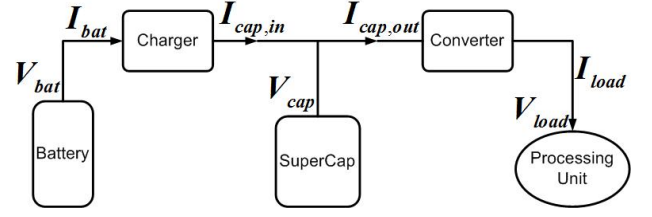


Fig. 1. The architecture of the portable embedded system with a hybrid power supply.

the mathematical formulation. More specifically, the relation between the battery OCV $V_{bat}^{OC}(t)$ and CCV $V_{bat}(t)$ is given by

$$V_{bat}(t) = V_{bat}^{OC}(t) - V_{tl}(t) - V_{ts}(t) - I_{bat}(t) \cdot R_s, \quad (1)$$

where $V_{tl}(t)$ and $V_{ts}(t)$ are the voltage drops across the internal capacitances, and R_s is the internal series resistance. The battery state-of-charge (SoC) $SoC(t)$ is defined as the ratio of the stored charge to the total charge when the battery is fully charged. For a Li-ion battery, the OCV-SoC relation is given as follows:

$$V_{bat}^{OC}(t) = b_1 \cdot e^{b_2 \cdot SoC(t)} + b_3 \cdot SoC^3(t) + b_4 \cdot SoC^2(t) + b_5 \cdot SoC(t) + b_6, \quad (2)$$

where those b_i are empirically determined parameters [8].

The rate capacity effect of batteries explains that the charging and discharging efficiencies decrease with the increase of charging and discharging currents, respectively. More precisely, the Peukert's Law [10] describes that the charging and discharging efficiencies of a battery as functions of the charging current I_c and discharging current I_d , respectively, are given by

$$\begin{aligned} \eta_{rate,c}(I_c) &= k_c / (I_c)^{\alpha_c}, \\ \eta_{rate,d}(I_d) &= k_d / (I_d)^{\alpha_d}, \end{aligned} \quad (3)$$

where k_c , α_c , k_d , and α_d are constants known *a priori*. We define the equivalent current inside the battery as the actual charge accumulating/reducing rate

$$I_{eq}(t) = \begin{cases} I_{bat}(t) / \eta_{rate,d}(I_{bat}(t)), & \text{if } I_{bat}(t) > 0, \\ I_{bat}(t) \cdot \eta_{rate,c}(|I_{bat}(t)|), & \text{if } I_{bat}(t) < 0. \end{cases} \quad (4)$$

Taking into account the rate capacity effect, the SoC of the battery can be calculated by

$$SoC(t) = SoC(T_{start}) - \frac{\int_{T_{start}}^t I_{eq}(\tau) d\tau}{C_{full}}, \quad (5)$$

where C_{full} in Coulomb is derived from the nominal battery capacity $Capacity$ given in Ahr:

$$C_{full} = 3600 \cdot Capacity. \quad (6)$$

B. Supercapacitor Model

The supercapacitor OCV and CCV are equal to each other since the internal resistance of a supercapacitor is negligible. For a supercapacitor, the OCV/CCV $V_{cap}(t)$ is a linear function of the amount of charge $Q_{cap}(t)$ stored in the supercapacitor. The rate capacity effect of supercapacitor is negligible, i.e., the

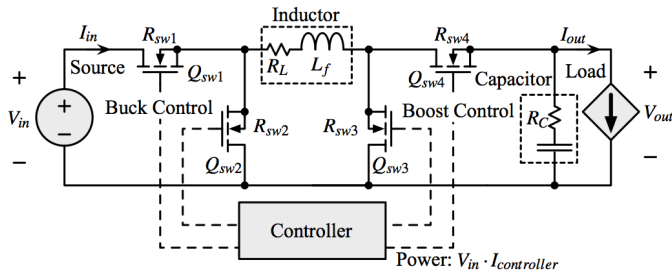


Fig. 2. The PWM buck-boost switching converter model.

charging and discharging efficiencies equal to one. A primary disadvantage of supercapacitor is the high self-discharge rate. A supercapacitor may lose more than 20% of its stored energy per day even if no load is connected to it [6]. The supercapacitor power loss due to self-discharge is given by

$$P_{sd}(t) = V_{cap}(t) \cdot I_{sd}(t) = C_{cap} \cdot (V_{cap}(t))^2 / \tau, \quad (7)$$

where $I_{sd}(t)$ is the self-discharge current, C_{cap} is the supercapacitor capacitance and τ is the self-discharge time constant. The supercapacitor stored charge is calculated by

$$Q_{cap}(t) = Q_{cap}(T_{start}) + \int_{T_{start}}^t (I_{cap,in}(\tau) - I_{cap,out}(\tau) - I_{sd}(\tau)) d\tau. \quad (8)$$

C. Power Converter Model

The charger and power converter used in the portable embedded system are PWM (pulse width modulation) buck-boost switching converters, which regulate their output current/voltage value into a desirable value according to the control algorithm. The model of a PWM buck-boost switching converter is shown in Fig. 2. The input voltage, input current, output voltage, and output current of the converter are denoted by V_{in} , I_{in} , V_{out} , and I_{out} , respectively. We use P_{conv} to denote the power loss of the converter, which includes the conduction loss, the switching loss and the controller loss [17], and we have:

$$P_{conv} = V_{in} \cdot I_{in} - V_{out} \cdot I_{out}. \quad (9)$$

Therefore, the power loss of the charger between the battery and the supercapacitor in Fig. 1 satisfies

$$P_{conv,in}(t) = V_{bat}(t) \cdot I_{bat}(t) - V_{cap}(t) \cdot I_{cap,in}(t). \quad (10)$$

And the power loss of the converter between the supercapacitor and the processing unit in Fig. 1 satisfies

$$P_{conv,out}(t) = V_{cap}(t) \cdot I_{cap,out}(t) - V_{load}(t) \cdot I_{load}(t). \quad (11)$$

Based on the relation between V_{in} and V_{out} , the converter has two possible working modes: the buck mode ($V_{in} > V_{out}$) and otherwise the boost mode. In the buck mode, the converter power loss P_{conv} is given by

$$P_{conv} = I_{out}^2 (R_L + D \cdot R_{sw1} + (1-D)R_{sw2} + R_{sw4}) + \frac{(\Delta I)^2}{12} (R_L + D \cdot R_{sw1} + (1-D)R_{sw2} + R_{sw4} + R_C) + V_{in} \cdot f_s (Q_{sw1} + Q_{sw2}) + V_{in} \cdot I_{controller}, \quad (12)$$

where $D = V_{out}/V_{in}$ is the PWM duty ratio and $\Delta I = V_{out}(1-D)/(L_f \cdot f_s)$ is the maximum current ripple; f_s is the switching frequency; $I_{controller}$ is the current flowing into the controller; R_L and R_C are the equivalent series resistances of the inductor L and the capacitor C , respectively; R_{swi} and Q_{swi} are the turn-on resistance and gate charge of the i -th MOSFET switch in Fig. 2, respectively.

In the boost mode, the power loss P_{conv} is given by

$$P_{conv} = \left(\frac{I_{out}}{1-D}\right)^2. \quad (13)$$

$$(R_L + D \cdot R_{sw3} + (1-D)R_{sw4} + R_{sw1} + D(1-D)R_C) + \frac{(\Delta I)^2}{12} (R_L + D \cdot R_{sw3} + (1-D)(R_{sw4} + R_C) + R_{sw1}) + V_{out} \cdot f_s (Q_{sw3} + Q_{sw4}) + V_{in} \cdot I_{controller},$$

where $D = 1 - V_{in}/V_{out}$ and $\Delta I = V_{in} \cdot D/(L_f \cdot f_s)$ in this case.

D. Processing Unit

We consider the operation of the portable embedded system from the time when the battery is fully charged till the time when it is fully depleted. The processing unit executes a set of N periodic tasks $\{\mathcal{T}_1, \mathcal{T}_2, \dots, \mathcal{T}_N\}$ with a common period of T_{period} . The time requirements to execute each instance of tasks $\mathcal{T}_1, \mathcal{T}_2, \dots, \mathcal{T}_N$ are denoted by T_1, T_2, \dots, T_N , respectively, satisfying $T_1 + T_2 + \dots + T_N < T_{period}$. The processing unit needs to execute an instance of each task in each time period. The supply voltage of the processing unit, i.e., V_{load} , is a fixed value, whereas the current of the processing unit, i.e., I_{load} , is equal to $I_{load,act}$ when it is executing a task and $I_{load,idle}$ when it is idle.

IV. JOINT CONTROL AND OPTIMIZATION ALGORITHM

In this work, we aim at maximizing the system service time. More specifically, at the beginning of the system operation, the battery is fully charged whereas the supercapacitor has zero (or low) charge. During the system operation, the processing unit executes periodic tasks as described in Section III-D, and no task dropping is allowed. We aim at maximizing the total number of finished task instances before the battery is depleted, which is equivalent to maximizing the system service time.

A. Motivations

We propose joint control and optimization of charging/discharging of the hybrid power supply with task scheduling in the embedded system based on the following two motivations:

Motivation I: The battery suffers from rate capacity effect as discussed in Section III-A, which specifies that the energy loss in the battery is a super-linear function of the battery's discharging current. The energy loss due to rate capacity effect will be minimized if the battery discharging current is nearly constant. As an example, the energy or charge loss in a battery with discharge current profile in Fig. 3(a) is higher than that in Fig. 3(b), although the average discharge current is the same.

Motivation II: The conversion efficiency of charger/power converter is not a constant value, but a variable depending

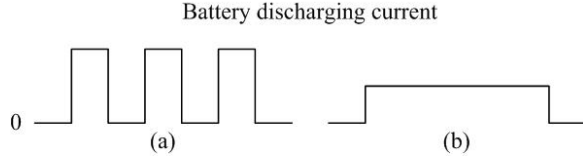


Fig. 3. An illustration of Motivation I.

on its input and output voltages and currents. In general, the power conversion efficiency will be maximized if its input and output voltages are close to each other. This leads to the motivation that a most desirable supercapacitor voltage $V_{cap,opt}$ exists, which results in the highest energy transfer efficiency or equivalently, the minimum energy loss in the battery in each task scheduling period.

Based on Motivation I, we are going to set the battery discharging current nearly constant. As a result, the system will operate in two modes. In Mode I, the processing unit is executing a task. In this case the supercapacitor mainly provides energy for the processing unit and we have $I_{cap,in}(t) < I_{cap,out}(t)$. In Mode II, the processing unit is idle and requires little amount of power. In this case the battery will charge the supercapacitor and we have $I_{cap,in}(t) > I_{cap,out}(t)$. The battery discharging currents in these two modes will be nearly the same.

Next we will discuss how to derive the most desirable supercapacitor voltage $V_{cap,opt}$. We assume that the supercapacitor voltage V_{cap} is constant (in order to derive $V_{cap,opt}$). We know that the processing unit will be busy for $\sum_{i=1}^N T_i$ amount of time in each period and will be idle for $T_0 = T_{period} - \sum_{i=1}^N T_i$ amount of time. Since the supercapacitor voltage is V_{cap} , we can calculate the supercapacitor discharging currents when the processing unit is busy and idle, denoted by $I_{cap,out,act}$ and $I_{cap,out,idle}$, respectively, based on the power converter model provided in Section III-C. Then we can estimate the (constant) supercapacitor charging current $I_{cap,in}$ using the following energy balancing equation:

$$V_{cap} \cdot I_{cap,in} \cdot T_{period} = V_{cap} \cdot (I_{cap,out,act} \cdot \sum_{i=1}^N T_i + I_{cap,out,idle} \cdot T_0) + V_{cap} \cdot I_{sd} \cdot T_{period}, \quad (14)$$

when the supercapacitor self-discharge is taken into account. After that we can derive the required battery discharging current I_{bat} based on the power converter model. Based on the above-mentioned calculation framework (i.e., from given V_{cap} to derive the required I_{bat}), we use the *ternary search algorithm* to find the optimal supercapacitor voltage $V_{cap,opt}$ that minimizes I_{bat} . The ternary search algorithm is an extension of the well-known binary search algorithm. The underlying assumption of the ternary search algorithm is that the battery discharging current I_{bat} is a quasi-convex function of supercapacitor voltage V_{cap} .

B. Joint Optimization Algorithm of Power Supply Control and Task Scheduling

The proposed joint optimization algorithm of power supply control and task scheduling is performed at the beginning

of each time period, i.e., $0, T_{period}, 2T_{period}, 3T_{period}, \dots$. The proposed algorithm is based on the feedback control technique (e.g., PID control), which could provide certain level of tolerance to control and model inaccuracies, to effectively control the supercapacitor voltage. We need to achieve the following two goals: (i) keep the battery discharging current nearly constant and (ii) keep the supercapacitor voltage near or above the most desirable value $V_{cap,opt}$. In the feedback control method, we also take into account the following two effects: (i) the optimal supercapacitor voltage $V_{cap,opt}$ also evolves, although slowly, due to the slow degradation of V_{bat}^{OC} during battery discharging², and (ii) the supercapacitor voltage is typically low at the beginning of system operation (because of its high self-discharge rate) and then we need to gradually increase the supercapacitor voltage towards the optimal value $V_{cap,opt}$ (maybe through multiple periods.)

At the beginning of each time period (suppose it is time $j \cdot T_{period}$ for $1 \leq j \leq N$), the current supercapacitor voltage level is given by $V_{cap}(j \cdot T_{period})$ while the battery OCV is $V_{bat}^{OC}(j \cdot T_{period})$. Then we execute the following three steps to perform joint control and optimization of the hybrid power supply and task scheduling in this time period:

Step I: Derive and update the optimal supercapacitor voltage $V_{cap,opt}(j \cdot T_{period})$ based on the current battery OCV $V_{bat}^{OC}(j \cdot T_{period})$, and set $V_{cap,opt}(j \cdot T_{period})$ as the new target value.

Step II: Schedule the set of tasks such that the supercapacitor terminal voltage can maintain nearly constant during the time period. More specifically, we need to interleave task execution and idle times as shown in Fig. 4.

Step III: With the given task scheduling from Step II, we derive the battery discharging current value during the time period, so that the supercapacitor terminal voltage will get closer to the target value $V_{cap,opt}(j \cdot T_{period})$ at the end of this time period based on the feedback control policy.

The procedure of Step I has already been described in Section IV.A, hence we elaborate Step II and Step III as follows:

Step II (task scheduling): In this step, we have the target supercapacitor voltage $V_{cap,opt}(j \cdot T_{period})$ derived from Step I. We assume that the supercapacitor voltage is $V_{cap,opt}(j \cdot T_{period})$ and is a constant value in the time period to derive the task scheduling. The assumption that the supercapacitor voltage is a constant value³ can effectively decouple the task scheduling problem with the derivation of battery discharge current I_{bat} . As shown in Fig. 4, the best way to schedule all tasks in a time period while maintaining the supercapacitor voltage nearly constant is to interleave the task execution and idle times of each task. More specifically, we execute \mathcal{T}_1 at the beginning of the time period, and then wait until the supercapacitor voltage returns to $V_{cap,opt}$. We subsequently execute \mathcal{T}_2 and wait, and go on this procedure until all task instances in the current time period have been executed. The ratio of task instance execution time of a task \mathcal{T}_i ($1 \leq i \leq N$)

²Note that the battery OCV is a monotonically increasing function of its SoC.

³Please note that this assumption is often valid because the supercapacitor voltage is around $V_{cap,opt}(j \cdot T_{period})$ when the system operation is stable.

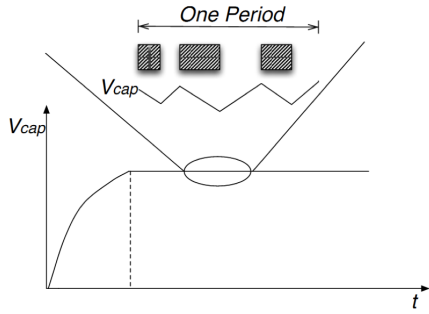


Fig. 4. An example showing the supercapacitor voltage control during system operation.

to the subsequent idle time is calculated by:

$$\frac{\sum_{i=1}^N T_i}{T_{period} - \sum_{i=1}^N T_i}. \quad (15)$$

Of course, this procedure is based on the ideal assumption that the supercapacitor voltage is $V_{cap,opt}(j \cdot T_{period})$ and has negligible change during task execution and idle times, which is not necessarily precise at the beginning of system operation and will inevitably result in control inaccuracy. This inaccuracy issue is effectively mitigated in Step III using the feedback control mechanism.

Step III (feedback control): In this step we have the task execution scheduling derived from Step II, and we are not going to change the task scheduling in this step. On the other hand, we are going to derive the battery discharging current I_{bat} during this time period, such that the supercapacitor terminal voltage will get closer to the target value $V_{cap,opt}(j \cdot T_{period})$ at the end of this time period using the feedback control policy. More specifically, the supercapacitor voltage should reach $(1 - \delta) \cdot V_{cap}(j \cdot T_{period}) + \delta \cdot V_{cap,opt}(j \cdot T_{period})$ at the end of this time period, where δ is a parameter specifying the speed to control the supercapacitor voltage.

We use the binary search method to find the appropriate I_{bat} value in this time period. There are two ways to implement the binary search algorithm. The first way uses $V_{cap}(j \cdot T_{period})$ and $V_{bat}^{OC}(j \cdot T_{period})$ as the approximations of the supercapacitor terminal voltage and battery OCV, respectively. There is inevitable modeling inaccuracy by using constant values to approximate these two voltages. However, such modeling inaccuracy could be effectively mitigated by the feedback control framework because of its inaccuracy tolerance capability. On the other hand, the second way accounts for changes in supercapacitor terminal voltage and battery OCV by dividing the whole time period into a number of fine-grained time slots and calculating the supercapacitor terminal voltage and battery OCV at the beginning of each time slot. The second way will result in a more accurate calculation of the I_{bat} value. Details of approaches are omitted due to space limitations.

Recall that as described in the beginning of Section IV-B, the proposed joint optimization algorithm needs to achieve two goals. The goal that the supercapacitor voltage is kept near the most desirable value is achieved by Step I (deriving the most desirable value) and Step III (using feedback control to maintain the voltage near the most desirable value.) Subsequently, the battery discharging current is nearly constant

because (i) we keep the discharging current constant in each time period and (ii) the battery discharging current will not change significantly among various time periods since the supercapacitor voltage is kept near the most desirable value. An example of joint control of hybrid energy supply and task scheduling is shown in Fig. 4. We show the system operation over multiple time periods. One can observe that the supercapacitor terminal voltage is initially low, and gradually increases thanks to the feedback control mechanism. We also see the task scheduling and supercapacitor terminal voltage change within a specific time period. We can see that although the supercapacitor terminal voltage drops during task execution and increases during idle time, the change is insignificant because task executions are interleaved and both the execution time of a task instance and the subsequent idle time are small compared to a time period or the total service time.

V. EXPERIMENTAL RESULTS

In this section we provide experimental results on the joint optimization framework of task scheduling and power supply control of the portable embedded system. For battery modeling, we obtain characteristics of Li-ion battery by performing measurement on a GP1051L35 Li-ion battery with 350 mAh nominal capacity [18], and extract parameters for the battery model described in Section III-A. We adopt a 5 F supercapacitor in the system, which is the typical size for embedded system applications. We apply Linear Technology LTM4607 converter as the converter and charger in the embedded system. We extract the parameters required in the converter model Eqns. (12) and (13) from the datasheet [19]. The supply voltage level of the embedded processing unit is 1.0 V. The static current of the processing unit $I_{load,idle}$ is 0.2 A, and we are going to change the active current $I_{load,act}$ when executing tasks in the experiments. We use one minute (60 seconds) as the time period for task scheduling.

We compare the performance of the proposed joint optimization framework with two baseline systems. The first baseline system only uses battery for power supply, without incorporating the supercapacitor. In this system the battery is connected to the embedded processing unit through a power converter. The second baseline system employs the same battery-supercapacitor hybrid system for power supply as the proposed system and same configurations. However, the second baseline system does not derive the optimal supercapacitor voltage and perform feedback control accordingly. Instead, it simply keeps the supercapacitor voltage as its initial value.

In the first experiment, we consider a set of 6 tasks with execution times (of each task instance) of 1 s, 1 s, 1.5 s, 1.5 s, 2 s, and 3 s, respectively. Fig. 5 illustrates the comparison results on the total service time (in minutes) between the proposed system and the two baseline systems. The X-axis of Fig. 5 is different active current values $I_{load,act}$'s of the processing unit, while the Y-axis is the total service time. One could observe that the proposed joint optimization framework consistently outperforms the two baseline systems, with the maximum improvements in total service time of 57% and 36%, respectively, when comparing with baseline 1 and baseline 2. Moreover, it can be observed that the improvement is more significant with higher $I_{load,act}$ values. This is because the more significant rate capacity effect degrades the performance of the baseline

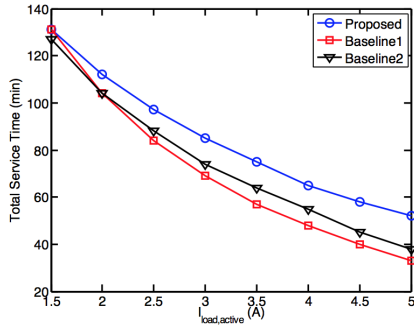


Fig. 5. The comparison results on the total service time (in minutes) between the proposed system and two baseline systems in the first experiment.

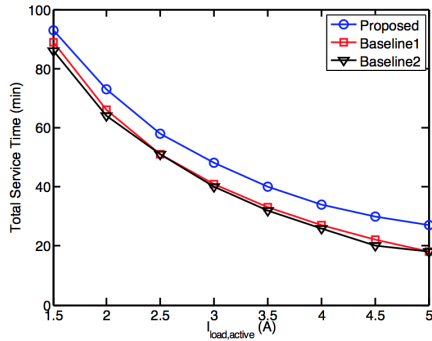


Fig. 6. The comparison results on the total service time (in minutes) between the proposed system and two baseline systems in the second experiment.

system, which could be effectively mitigated by the proposed system through maintaining the battery discharging current nearly constant.

In the second experiment, we consider a set of 6 tasks with execution times (of each task instance) of 2 s, 2 s, 3 s, 3 s, 4 s, and 6 s, respectively. In fact, the execution time of each task instance is twice of that in the first experiment. Fig. 6 illustrates the comparison results on the total service time (in minutes) between the proposed system and the two baseline systems. Similar to the first experiment, the proposed joint optimization framework consistently outperforms the two baseline systems, and the improvement is more significant when the $I_{load,act}$ value is higher. Moreover, when comparing with the first experiment, we observe that the improvement of the proposed optimization framework over baselines is slightly lower than the improvement in the first experiment. This is because the battery in the proposed system also suffers from rate capacity effect when the execution times of task instances become longer.

VI. CONCLUSION

Energy efficiency has always been an important design criterion for portable embedded systems. To compensate for the shortcomings of electrochemical batteries such as low power density, limited cycle life, and rate capacity effect, supercapacitors have been employed as complementary power supplies, i.e., hybrid power supplies comprised of batteries and supercapacitors have been proposed. In this work, we consider a portable embedded system with a hybrid power supply

and executing periodic real-time tasks. We perform system power management from both the power supply side and the power consumption side to maximize the system service time. Specifically, we use feedback control for maintaining the supercapacitor energy at a certain level by regulating the discharging current of the battery, such that the supercapacitor has the capability to buffer the load current fluctuation. At the power consumption side, we perform task scheduling to assist supercapacitor energy maintenance.

REFERENCES

- [1] Y. H. Lu, L. Benini, and G. De Micheli, "Low-power task scheduling for multiple devices," in *Proc. of the 8th Int'l Workshop on Hardware/Software Codesign*, 2000, pp. 39-43.
- [2] Q. Qiu, S. Liu, and Q. Wu, "Task merging for dynamic power management of cyclic applications in real-time multi-processor systems," in *Proc. of Int'l Conference on Computer Design (ICCD)*, 2006, pp.397-404.
- [3] F. Yao, A. Demers, and S. Shenker, "A scheduling model for reduced CPU energy," in *Proc. of the 36th Annual Symposium on Foundations of Computer Science*, 1995, pp. 374-382.
- [4] G. Quan and X. S. Hu, "Minimal energy fixed-priority scheduling for variable voltage processors," *IEEE Trans. Computer-Aided Design of Integrated Circuits and Systems*, vol. 22, pp. 1062-1071, Aug. 2003.
- [5] S. Park, Y. Kim, and N. Chang, "Hybrid energy storage systems and battery management for electric vehicles," in *Proc. of the 50th Design Automation Conference (DAC)*, 2013, pp. 1-6.
- [6] M. Pedram, N. Chang, Y. Kim, and Y. Wang, "Hybrid electrical energy storage systems," in *Proc. of Int'l Symposium on Low-Power Electronics and Design (ISLPED)*, 2010, pp. 363-368.
- [7] F. Koushanfar, "Hierarchical hybrid power supply networks," in *Proc. of the 47th Design Automation Conference (DAC)*, 2010, pp. 629-630.
- [8] D. Shin, Y. Kim, J. Seo, N. Chang, Y. Wang, and M. Pedram, "Battery-supercapacitor hybrid system for high-rate pulsed load applications," in *Proc. of Design, Automation & Test in Europe Conference & Exhibition (DATE)*, 2011, pp. 1-4.
- [9] P. Rong and M. Pedram, "Battery-aware power management based on markovian decision processes," in *Proc. of Int'l Conference on Computer-Aided Design (ICCAD)*, 2002, pp. 707-713.
- [10] X. Jiang, J. Polastre, and D. Culler, "Perpetual environmentally powered sensor networks," in *Proc. of Int'l Symposium on Information Processing in Sensor Networks (IPSN)*, 2005, pp. 463-468.
- [11] C. Park and P. H. Chou, "AmbiMax: autonomous energy harvesting platform for multi-supply wireless sensor nodes," in *Proc. of the 3rd Annual IEEE Communications Society on Sensor and Ad Hoc Communications and Networks (SECON)*, 2006, pp. 168-177.
- [12] A. Mirhoseini and F. Koushanfar, "HypoEnergy: hybrid supercapacitor-battery power-supply optimization for energy efficiency," in *Proc. of Design, Automation & Test in Europe Conference & Exhibition (DATE)*, 2011, pp.1-4.
- [13] A. Mirhoseini and F. Koushanfar, "Learning to manage combined energy supply systems," in *Proc. of Int'l Symposium on Low-Power Electronics and Design (ISLPED)*, 2011, pp. 229-234.
- [14] S. Yue, D. Zhu, Y. Wang, and M. Pedram, "Reinforcement learning based dynamic power management with a hybrid power supply," in *Proc. of Int'l Conference on Computer Design (ICCD)*, 2012, pp. 81-86.
- [15] M. Chen and G. A. Rincon-Mora, "Accurate electrical battery model capable of predicting runtime and I-V performance," *IEEE Trans. Energy Conversion*, vol. 21, pp. 504-511, Jun. 2006.
- [16] D. Linden and T. B. Reddy, *Handbook of Batteries*. McGraw-Hill Professional, 2001.
- [17] Y. Wang, Y. Kim, Q. Xie, N. Chang, and M. Pedram, "Charge migration efficiency optimization in hybrid electrical energy storage (HEES) systems," in *Proc. of Int'l Symposium on Low-Power Electronics and Design (ISLPED)*, 2011, pp. 103-108.
- [18] *Gold Peak Industries, GP batteries datasheet: Model GP1051L35*.
- [19] *Linear Technology, LTM4607: 36 V in, 24 V out high efficiency buck-boost DC/DC MicroModule*, 2008.